

Research Article

Effect of Double Stratification on MHD Williamson Boundary Layer Flow and Heat Transfer across a Shrinking/Stretching Sheet Immersed in a Porous Medium

R. Geetha ¹, B. Reddappa ¹, Nainaru Tarakaramu ², B. Rushi Kumar ³
and M. Ijaz Khan ⁴

¹Department of Mathematics, School of Advanced Sciences, Kalasalingam Academy of Research and Education (Deemed to be University), Anand Nagar, Krishnankoil 626126, Virudhunagar, Tamil Nadu, India

²Department of Mathematics, School of Liberal Arts and Sciences,

Mohan Babu University (Erstwhile Sree Vidyanikethan Engineering College), Sree Sainath Nagar, Tirupati 517102, AP, India

³Department of Mathematics, School of Advanced Sciences, Vellore Institute of Technology, Vellore, Tamil Nadu 632014, India

⁴Department of Mechanical Engineering, Lebanese American University, Kraytem 1102-2801, Beirut, Lebanon

Correspondence should be addressed to B. Reddappa; drreddappa@gmail.com and M. Ijaz Khan; scientificresearchglobe@gmail.com

Received 15 February 2024; Revised 9 March 2024; Accepted 30 April 2024; Published 15 May 2024

Academic Editor: Jitendra Kumar

Copyright © 2024 R. Geetha et al. This is an open access article distributed under the Creative Commons Attribution License, which permits unrestricted use, distribution, and reproduction in any medium, provided the original work is properly cited.

The present study aims to provide a mathematical model of the Williamson fluid flow via a permeable stretching/shrinking sheet in the MHD boundary layer in the presence of a heat source, chemical reaction, and suction. This study is novel because it investigates the physical effects of thermal and solutal stratification on convective heat and mass transport using thermal radiation. The flow's PDEs are numerically solved using the BVP4c approach and the pertinent similarity variables until a stable solution is found. Through visual analysis, the effects of dimensionless factors on temperature, velocity, and concentration profiles are examined. This encompasses the mass transfer rate, the heat transfer rate, and the coefficient of friction. The results of the present analysis are found to be consistent with those of previously published studies. The findings demonstrate that enhanced temperature and concentration profiles cause the Williamson, magnetic, and permeability parameters to rise in conjunction with a drop in the dimensionless velocity. In relation to temperature, the thermal stratification parameter exhibits the opposite tendency. Regarding the solutal stratification parameter, concentration profiles are seen to show the opposite trend. Lastly, the current work will have important implications for the removal of dust and viruses from viscoelastic fluid in bioengineering, the medical sciences, and medical equipment.

1. Introduction

Non-Newtonian fluids may be classified as pseudoplastic Williamson fluids. As its practical uses and inherent interest grow, the field of research known as boundary layer flow in pseudoplastic fluids is growing in prominence. The power law model, the Carreaus model, the Cross model, and the Ellis model are only some of the better examples of mathematical frameworks that may be used to explain the behaviour of pseudoplastic fluids. Williamson studied the behaviour of pseudoplastic fluids and proposed an equation-based model to

define their motion in 1929. There have been empirical confirmations of this idea ever since. Williamson fluid peristaltic flow in a vertical annulus was investigated for its impact on heat and mass transmission by Nadeem and Sher Akbar [1]. In an asymmetric tube with porous walls, Vajravelu et al. reported the peristaltic motion of a Williamson fluid [2]. The Williamson fluid model and its many uses in studying fluid dynamics are presented. The Williamson fluid injection into a rock fracture perturbation solution was described by Dapra and Scarpi [3]. Khan and Khan [4] investigated many approaches to four flow issues using a Williamson fluid by employing the homotopy

analysis method (HAM). Williamson fluid flow over a linear and exponentially stretched surface has been modelled in two dimensions by Nadeem et al. [5]. Hayat et al. explored the time-independent MHD flow of Williamson fluid across a porous plate and found a solution with a number of phases [6]. The flow of a non-Newtonian fluid through a pipe with variable permeability and an inclined plane was taken into consideration by the authors Bandi et al. [7]. Sudheer Babu et al. [8] investigated the impact of chemical reactions on MHD heat and mass transfer in a Jeffrey fluid flow with viscous dissipation and joule heating. They used a porous stretched sheet.

The existence of many fluids, fluctuations in temperature, or both may all contribute to fluid stratification. Natural convection in a doubly stratified medium is a fascinating and vital area of research owing to its wide range of practical applications in engineering. Thermal sources include the condensers in power plants, whereas thermal energy storage techniques include solar ponds. Heat may also be dissipated into bodies of water like lakes, rivers, and seas using this method. The impact of medium stratification on the process of removing heat from a fluid has not gotten much attention in the literature despite its significance. Jumah and Mujumdar [9] examined free convection heat and mass transfer away from a vertical flat plate in saturated porous media for non-Newtonian power law fluids under yield stress. Murthy et al. [10] looked at how double stratification affected free convection heat and mass transfer in a porous Darcian fluid-saturated medium with uniform wall heat and mass flow. Lakshmi Narayana and Murthy [11] investigated free convection heat and mass transport away from a vertical flat plate in a doubly stratified non-Darcy porous material using the series solution technique. Cheng [12] considered the natural convection flow from a vertical wavy surface in a power-law fluid-saturated porous medium with temperature and mass stratification. Narayana et al. [13] studied free convection heat and mass transport in multilayer porous media saturated with a power-law fluid.

Analysis of heat along with the mass transfer on fluids over an exponentially extending surface with chemical reaction impact has a crucial role in nuclear reactors, aeronautics, drying procedures, cosmic fluid dynamics, heat exchangers, geothermal, chemical engineering, building construction, solar physics, solar collectors, and also oil recovery. Many researchers [14–18] are assessed over chemical reactions over a stretching sheet. Kumar et al. [19] studied the effects of Soret, DuFour, hall current, and rotation on MHD natural convective heat and mass transfer flow past an accelerated vertical plate through a porous medium. Goud et al. [20] analysed the thermal radiation and Joule heating effects on a magnetohydrodynamic Casson nanofluid flow in the presence of chemical reaction through a nonlinear inclined porous stretching sheet. Reddy et al. [21] investigated the effect of heat generation/absorption on MHD copper-water nanofluid flow over a nonlinear stretching/shrinking sheet. MHD boundary layer flow of nanofluid and heat transfer has been studied by the authors in [22–25]. Unsteady MHD free convective flow past a vertical porous plate with variable suction discussed by Srinivasa Raju et al. [26]. The researchers whose studies the

writers evaluated included Al-Ajmi and Mosaad [27], Hamimid et al. [28], Choukairy and Bennacer [29], Labeled et al. [30], and Ram and Bhandari [31]. Reddappa et al. [32], Krishnamurthy et al. [33], Krishna et al. [34], Khan et al. [35], Chetteti and Srivastav [36], Yousef et al. [37], Shaheen et al. [38], and Ananthaswamy et al. [39] studied double-stratification Jeffrey flow, MHD free convection, and the influence of second-order chemical processes in a porous material across an exponentially stretched sheet.

A fluid system that displays two separate layers of stratification, usually in relation to temperature or concentration gradients, is referred to as double stratified. All properties of a fluid, including density, temperature, or concentration, that vary or layer with regard to depth are referred to as stratification. In order to create a more complex stratified structure, double stratification indicates that the fluid contains two distinct gradients or variations. Heat transfer across a shrinking/stretching sheet submerged in a porous medium, and the MHD Williamson boundary layer flow is examined in the setting of double stratification. This allows for an examination of the consequences of additional complexity in the fluid system. With separate gradients for each stratified layer, the temperature or concentration distribution is altered, while additional buoyancy effects are added. Understanding the effects of double stratification is essential to accurately portraying the physical processes occurring in the system. There may not have been enough research done on the effects of two-fold stratification in the context of MHD Williamson boundary layer flow with a shrinking/stretching sheet immersed in a porous medium. The existing research may focus primarily on single stratification situations or flow configurations.

The necessity of employing various non-Newtonian fluids to store thermal energy has led to a significant increase in the use of Williamson fluid. The Williamson fluid model may provide a starting point for analyzing shear-thinning fluids, and it has limitations when applied to complex fluid dynamics problems involving double stratification, MHD, and heat transfer across porous media. A collection of partial differential equations (PDEs) that are nonlinear express the flow mathematically. The governing equations are converted into a set of ordinary differential equations (ODEs) with the necessary boundary conditions using similarity transformations, which can then be numerically solved using MATLAB's built-in solver `bvp4c`. The profiles of velocity, temperature, and concentration have been graphically shown and tabulated, along with the effects of changing the parameters that control the flow. The findings show that the stratification parameter significantly affects the flow field when wall suction is present. This research also includes an evaluation of the heat transfer coefficient from the perspective of industrial applications. The findings are expected to advance the body of knowledge and have real-world applications from earlier research.

2. Fluid Model

For Williamson fluid model, Cauchy stress tensor \bar{S} is defined as [40].

$$\bar{S} = -p\bar{I} + \bar{\tau}, \quad (1)$$

$$\bar{\tau} = \left(\mu_{\infty} + \frac{\mu_0 - \mu_{\infty}}{1 - \Gamma\dot{\gamma}} \right) \bar{A}_1, \quad (2)$$

where \bar{S} is extra stress tensor, μ_0 is limiting viscosity at zero shear rate and μ_{∞} is limiting viscosity at infinite shear rate, $\Gamma > 0$ is a time constant, \bar{A}_1 is the first Rivlin–Erickson tensor, and $\dot{\gamma}$ is defined as follows:

$$\dot{\gamma} = \sqrt{\frac{1}{2}\pi}, \quad \pi = \text{trace}(A_1^2). \quad (3)$$

Here, we considered the case for which $\mu_{\infty} = 0$ and $\Gamma\dot{\gamma} < 1$. Thus, $\bar{\tau}$ can be written as

$$\bar{\tau} = \left(\frac{\mu_0}{1 - \Gamma\dot{\gamma}} \right) \bar{A}_1. \quad (4)$$

By using binomial expansion, we get

$$\bar{\tau} = \mu_0 (1 - \Gamma\dot{\gamma}) \bar{A}_1. \quad (5)$$

3. Formulation of the Problem

Consider the motion of a stretched sheet in a Williamson fluid that is incompressible, viscous, and electrically conductive. The stretched sheet is enclosed in a porous material; therefore, it is assumed that the fluid is flowing through it k' . Assumptions about the fluid content along the sheet C_w and the sheet temperature are made in a similar vein $y = 0$ is T_w . The fluid is flowing smoothly and has a somewhat low viscosity. The boundary layer region, which is the thin layer adjacent to the sheet surface, appears to be the zone where the modifying influence is least likely to occur. Within such a layer, the fluid velocity rapidly changes from its starting value to the mainstream value. This model was selected because it offers a decent approximation of the behavior of various non-Newtonian fluids over a wide range of shear rates. The origin is located at the leading edge of the sheet, and the y -axis is perpendicular to the x -axis, which is selected to be parallel to the surface of the sheet in the flow direction. B is a magnetic field that has been applied perpendicular to the flow direction. The induced magnetic field will be much smaller than the applied magnetic field, assuming that the fluid has some conductivity (Figure 1), and the magnetic Reynolds number will be much lower than unity. Let T stand for the fluid's temperature, u and v for the perpendicular velocity, and represent the x -axial velocity. According to this hypothesis, the temperature and mass concentration of the surrounding medium are linearly stratified and take the form of $T = T_w = T_0 + a_1x$, $C = C_w = C_0 + b_1x$ and $T_{\infty} = T_0 + a_2x$, $C_{\infty} = C_0 + b_2x$. The initial ambient temperature and concentration are represented by T_w , T_{∞} and C_w , C_{∞} , and the constants a_1 , a_2 , b_1 , and b_2 are used to vary the intensity of stratification in the medium.

The continuity, momentum, energy, and concentration equations [41] control such a flow.

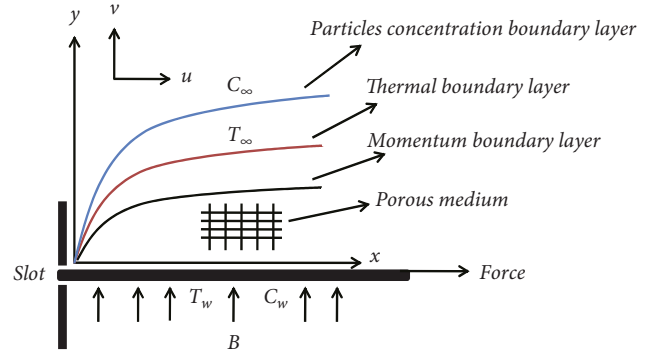


FIGURE 1: The system for coordinating flows.

$$\frac{\partial u}{\partial x} + \frac{\partial v}{\partial y} = 0, \quad (6)$$

$$u \frac{\partial u}{\partial x} + v \frac{\partial u}{\partial y} = v \frac{\partial^2 u}{\partial y^2} + \sqrt{2} v \Gamma \frac{\partial u}{\partial y} \frac{\partial^2 u}{\partial y^2} - \frac{\sigma B^2}{\rho} u - \frac{v}{k'} u, \quad (7)$$

$$u \frac{\partial T}{\partial x} + v \frac{\partial T}{\partial y} = \frac{k}{\rho c_p} \frac{\partial^2 T}{\partial y^2} + \frac{Q}{\rho c_p} (T - T_{\infty}), \quad (8)$$

$$u \frac{\partial C}{\partial x} + v \frac{\partial C}{\partial y} = D \frac{\partial^2 C}{\partial y^2} - k_r (C - C_{\infty}), \quad (9)$$

where u and v are the components of velocity in the x and y directions, respectively, $v = \mu/\rho$ denotes kinematic fluid velocity, ρ denotes fluid density, μ is the coefficient of fluid viscosity, Γ stands for a Williamson time constant, k' is the permeability of the porous medium, T and T_{∞} , respectively, are fluid temperature and ambient fluid temperature, Q is the heat source parameter. A uniform magnetic field of strength B is applied in the transverse direction of the flow; due to the small magnetic Reynolds number, it is not necessary to introduce the effect of the induced magnetic field. c_p signifies the specific heat at constant pressure, k_r is the reaction rate, D is the diffusion coefficient, and C_{∞} is the ambient fluid concentration.

Constraint set for boundary is [42]

$$\begin{aligned} u &= U_w, \\ v &= -v_w, \\ T &= T_w = T_0 + a_1x, \\ C &= C_w = C_0 + b_1x \text{ at } y = 0 \\ u &\longrightarrow 0, \\ T &\longrightarrow T_{\infty} = T_0 + a_2x, \\ C &\longrightarrow C_{\infty} = C_0 + b_2x \text{ as } y \longrightarrow \infty, \end{aligned} \quad (10)$$

where $U_w = cx$ for the case of a stretched sheet and $U_w = -cx$ for the case of a contracting sheet, with $c > 0$ the amount of contraction or expansion held constant. $v_w > 0$ speed at which mass is transferred over a wall in preparation $v_w > 0$ for mass injection $v_w < 0$ or mass suction.

Similarity transformations are [43]

$$\begin{aligned}\psi &= \sqrt{c\nu} x f(\eta), \eta = y \sqrt{\frac{c}{\nu}}, \\ T &= T_\infty + \theta(\eta)(T_w - T_0), \\ C &= C_\infty + \phi(\eta)(C_w - C_0),\end{aligned}\quad (11)$$

where ψ is the stream function and η is the similarity variable.

Stream functions are given by

$$\begin{aligned}u &= \frac{\partial \psi}{\partial y} \quad \text{and} \\ v &= -\frac{\partial \psi}{\partial x}.\end{aligned}\quad (12)$$

From equations (11) and (12), the suitable similarity transforms are

$$\begin{aligned}u &= cx f'(\eta), \\ v &= -\sqrt{c\nu} f(\eta), \\ T &= a_1 x \theta(\eta), \\ T_\infty &= T_0 + a_2 x, \\ C &= b_1 x \phi(\eta), \\ C_\infty &= C_0 + b_2 x.\end{aligned}\quad (13)$$

Equations (7)–(9) can be simplified by applying the aforementioned similarity modifications.

$$f''' + Wi f'' f''' + f f'' - f'^2 - (M + \lambda_2) f' = 0, \quad (14)$$

$$\theta'' + Pr f \theta' - Pr f' \theta - Pr e_1 f' + Pr \gamma \theta = 0, \quad (15)$$

$$\phi'' + Sc (f \phi' - f' \phi - K_1 \phi - e_2 f') = 0. \quad (16)$$

The following are the flow's relevant boundary conditions:

$$\begin{aligned}f &= S, \\ f' &= 1, \\ \theta &= 1 - e_1, \\ \phi &= 1 - e_2 \text{ at } \eta = 0 \\ f' &= 0, \\ \theta &= 0, \\ \phi &= 0 \text{ as } \eta \rightarrow \infty,\end{aligned}\quad (17)$$

where $Wi = \Gamma x \sqrt{2c^3/\nu}$ is the non-Newtonian Williamson parameter, $M = (\sigma B_0^2/\rho c)$ is the magnetic parameter, $\lambda_2 = \nu/k'c$ is the permeability parameter, $Pr = \mu c_p/k$ is the Prandtl number, $e_1 = a_2/a_1$ is the thermal stratification parameter, $\gamma = Q/c\rho c_p$ is the heat generation/absorption parameter, $Sc = \nu/D$ is the Schmidt number, $e_2 = b_2/b_1$ is the

solutal stratification parameter, $K_1 = k_r/c$ is the chemical reaction parameter, and $S = \nu_w/\sqrt{c\nu}$ is the wall mass parameter (with $S > 0$ (i.e., $\nu_w > 0$) wall mass suction and $S < 0$ (i.e., $\nu_w < 0$) wall mass injection).

Furthermore, the drag force coefficient in terms of C_f , the local Nusselt number Nu , and the local Sherwood number Sh are determined by [43]

$$\begin{aligned}C_f &= \frac{\tau_w}{\rho U_w^2} \frac{\partial u}{\partial y} \Big|_{y=0}, \\ Nu_x &= -\frac{x}{(T_w - T_\infty)} \frac{\partial T}{\partial y} \Big|_{y=0}, \\ Sh_x &= -\frac{x}{(C_w - C_\infty)} \frac{\partial C}{\partial y} \Big|_{y=0},\end{aligned}\quad (18)$$

by introducing the transformations (11) and (12), we have

$$\begin{aligned}\sqrt{Re_x} C_f &= \left(f''(0) + \frac{Wi}{2} (f''(0))^2 \right), \\ \frac{Nu}{\sqrt{Re_x}} &= -\theta'(0), \\ \frac{Sh}{\sqrt{Re_x}} &= -\phi'(0),\end{aligned}\quad (19)$$

where $Re_x = U_w x/\nu$ is the local Reynolds number.

4. Methodology

The BVP4c technique is a numerical method used to solve boundary value problems (BVPs). BVP involves finding a solution to a differential equation that satisfies specified boundary conditions. The BVP4c technique provides a robust and efficient way to solve BVPs numerically by discretizing the problem, formulating and solving the resulting system of equations, and incorporating the specified boundary conditions (Figure 2)

Adding new variables to transform higher-order differential equations into linear equations,

$$f_1 = f, f_2 = f', f_3 = f'', f_4 = \theta, f_5 = \theta', f_6 = \phi, f_7 = \phi'. \quad (20)$$

Equations (14)–(16) are transformed into the following the first-order ODE.

$$\begin{aligned}f_2' &= f_3, f_3' = \frac{1}{(1 + Wi f_3)} (-f_1 f_3 + f_2^2 + (M + \lambda_2) f_2), \\ f_4' &= f_5, f_5' = -Pr (f_1 f_5 - f_2 f_4 - e_1 f_2 + \gamma f_4), \\ f_6' &= f_7, f_7' = -Sc (f_1 f_7 - f_2 f_6 - K_1 f_6 - e_2 f_2),\end{aligned}\quad (21)$$

with the boundary conditions:

$$f_a(1) = S, f_a(2) = 1, f_a(4) = 1 - e_1, f_a(6) = 1 - e_2, f_b(2) = 0, f_b(4) = 0, f_b(6) = 0, \quad (22)$$

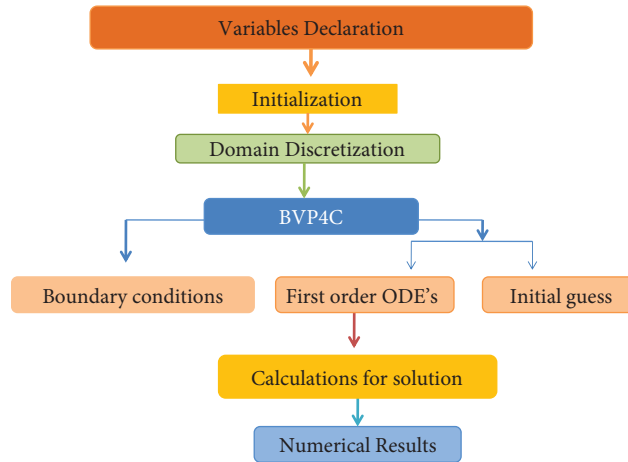


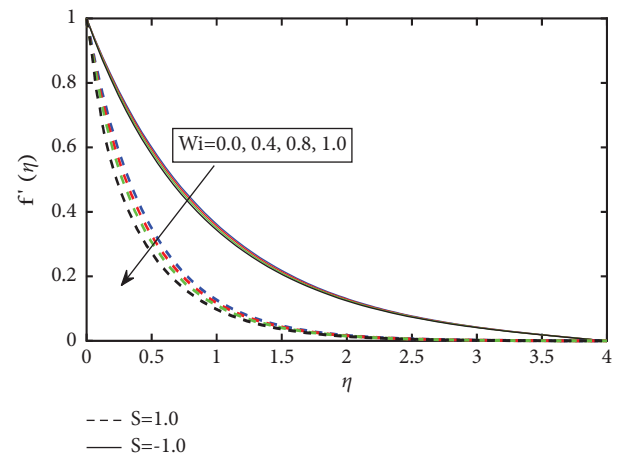
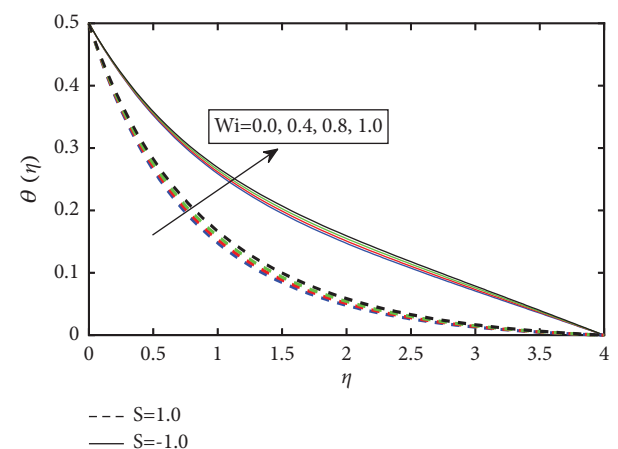
FIGURE 2: Step by step numerical procedure.

with the use of MATLAB `bvp4c` programming, approximate solutions are numerically calculated to show the practical importance of nondimensional quantities.

5. Results and Discussion

Numerical calculations have been made using the technique outlined in the preceding section for a variety of variables in order to assess the findings like wall mass parameter (S), Williamson parameter (Wi), magnetic parameter (M), permeability parameter (λ_2), Prandtl number (Pr), thermal stratification parameter (e_1), heat generation/absorption parameter (γ), Schmidt number (Sc), chemical reaction parameter (K_1), and solutal stratification parameter (e_2). For illustrations of the results, numerical values are plotted in Figures 3–17.

Table 1 compares the current findings with the body of prior research in a few selected examples. The current results and the body of literature showed higher agreement, we discovered. This demonstrates the reliability of the results as well as the precision of the numerical method we employed in this investigation. Table 2 displays the values for the skin friction coefficient, Nusselt number, and Sherwood number for a range of relevant parameter values. As magnetic parameter M , permeability parameter λ_2 , and thermal stratification parameter e_1 are increased, research demonstrates that an increase in the Williamson parameter Wi results in an increase in the skin friction coefficient; however, the trend is the opposite for the Sherwood number and the Nusselt number. It is evident that the skin friction coefficient, Nusselt number, and Sherwood number decrease. As increase in the wall mass parameter S , the skin friction coefficient results to decrease, whereas an opposite behaviour is noticed in Nusselt number and Sherwood number. As increase in solutal stratification parameter e_2 , it can be seen that the Nusselt number augments, while the Sherwood number shows the reverse pattern. The Nusselt number increases as the Prandtl number Pr rises, according to observations, although the heat generation/absorption parameter γ exhibits the reverse pattern. It is evident that when

FIGURE 3: Outcome of Wi on velocity profiles.FIGURE 4: Outcome of Wi on temperature profiles.

the parameters for chemical reactions K_1 and Schmidt number Sc rise, the Sherwood number amplifies.

The results of the Williamson parameter on the concentration, temperature, and velocity profiles during

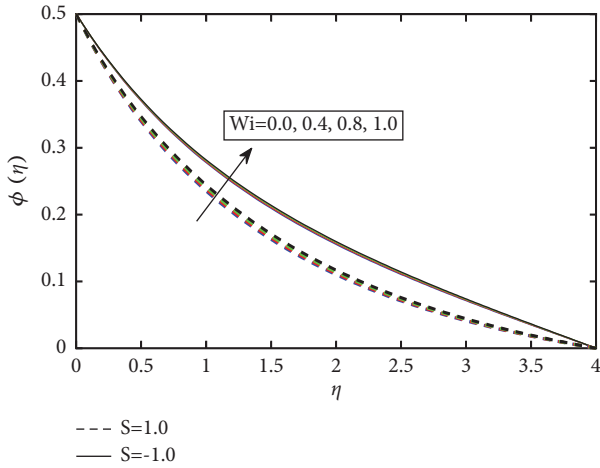


FIGURE 5: Outcome of Wi on concentration profiles.

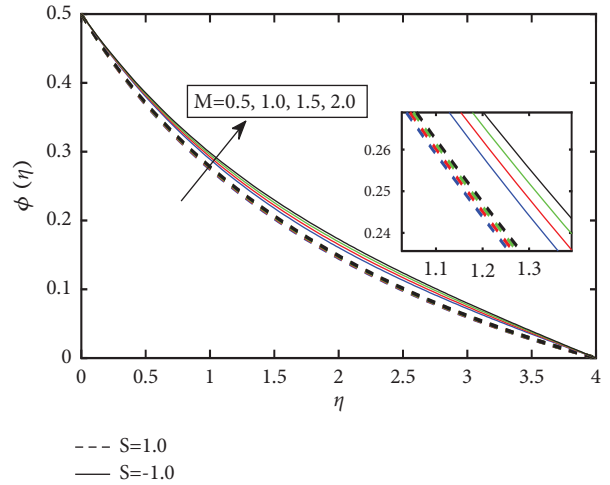


FIGURE 8: Outcome of M on concentration profiles.

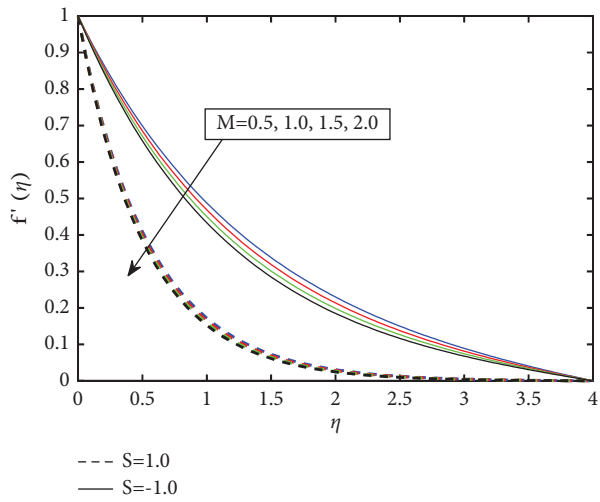


FIGURE 6: Outcome of M on velocity profiles.

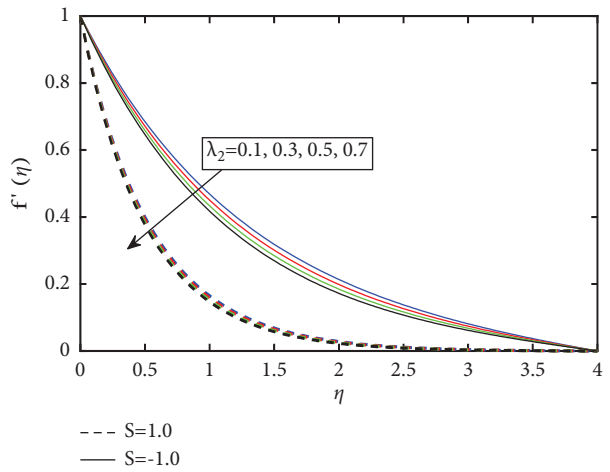


FIGURE 9: Outcome of λ_2 on velocity profiles.

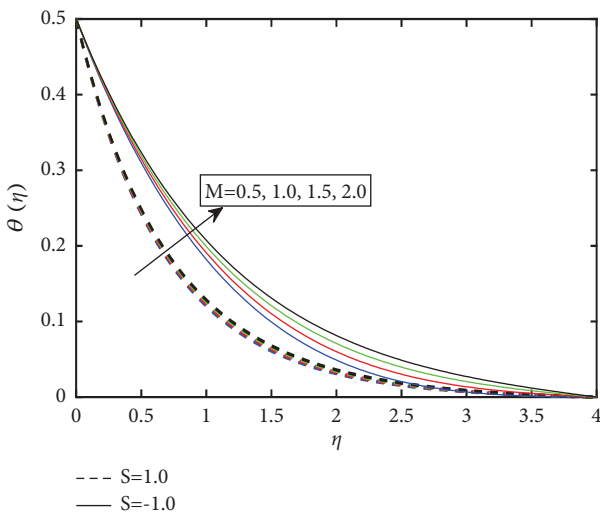


FIGURE 7: Outcome of M on temperature profiles.

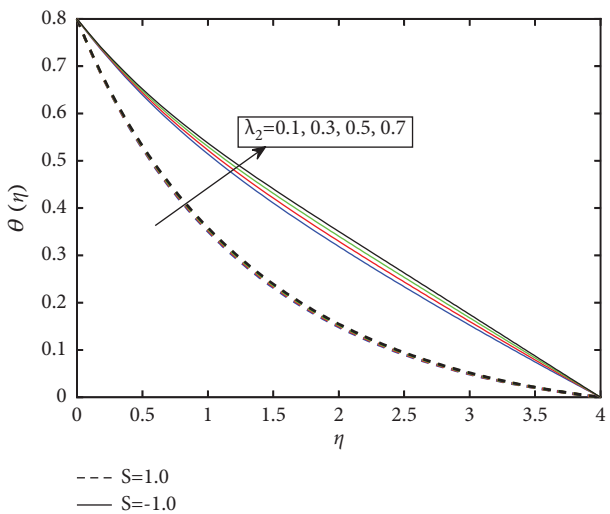


FIGURE 10: Outcome of λ_2 on temperature profiles.

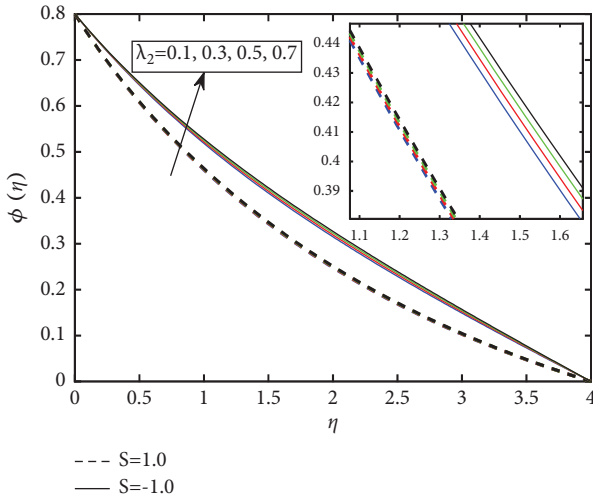


FIGURE 11: Outcome of λ_2 on concentration profiles.

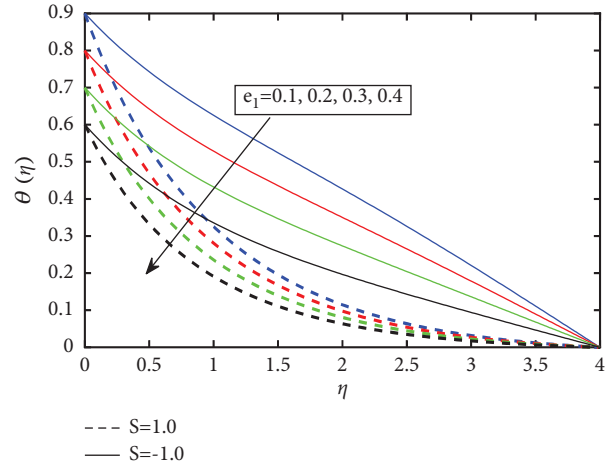


FIGURE 13: Outcome of e_1 on temperature profiles.

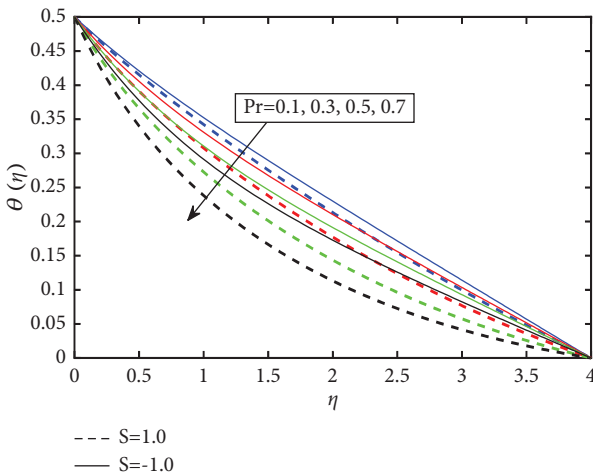


FIGURE 12: Outcome of Pr on temperature profiles.

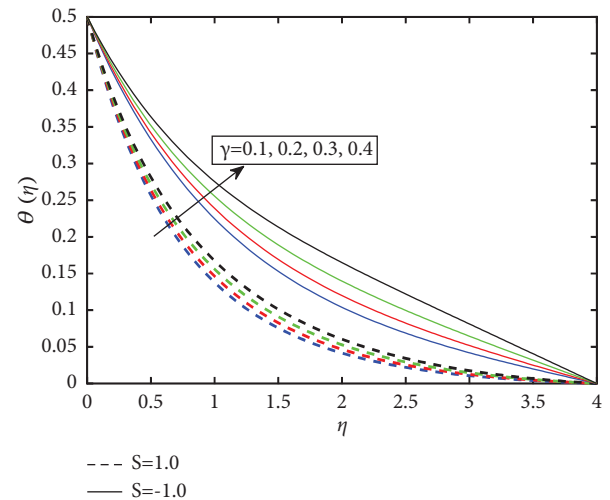


FIGURE 14: Outcome of γ on temperature profiles.

expansion and contraction are shown in Figures 3–5. The graph shows that increasing Wi causes fluid velocity to drop, while increasing Wi causes temperature and concentration distributions to climb. Physically, a higher Wi decreases the fluid’s velocity and enhances the fluid’s heat distribution through the boundary layer by increasing the viscous forces that hold the Williamson fluid layers together. Fluid motion is impeded by the extended relaxing time. In physical studies of viscoelastic flows, the Wi is used to measure the contribution of elastic to viscous forces.

The temperature, concentration, and velocity profiles for the shifting magnetic parameter during expansion and contraction are shown in Figures 6–8, respectively. As M increases, it is found that the fluid’s velocity drops. However, the Lorentz force, which acts against fluid motion, increases with M , so the transport rate actually decreases with M . However, when it is kept constant, the fluid temperature and concentration distributions grow M , leading to a thicker thermal boundary layer.

In Figures 9–11, we see the profiles of velocity, temperature, and concentration as a function of the permeability parameter for both the expanding and contracting cases. In both cases, the results improve with decreasing velocity λ_2 . The temperature and concentration profiles act differently for different values of λ_2 . The fluid temperature was shown to rise with an increasing porosity parameter. The same behaviours occur when concentrating a fluid. In Figures 9–11, we see the profiles of velocity, temperature, and concentration as a function of the permeability parameter for both the expanding and contracting cases. In both cases, the results improve with decreasing velocity. The temperature and concentration profiles act differently for different values. The fluid temperature was shown to rise with increasing porosity parameter. The same behaviours occur when concentrating a fluid. The physical effect of the porosity is to slow the flow of fluids and increase the temperature and concentration gradients across the material. In either the expanding or contracting situation, a large increase in the

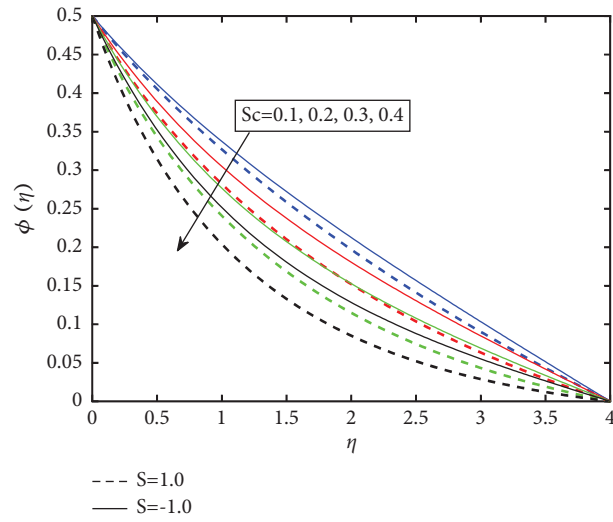
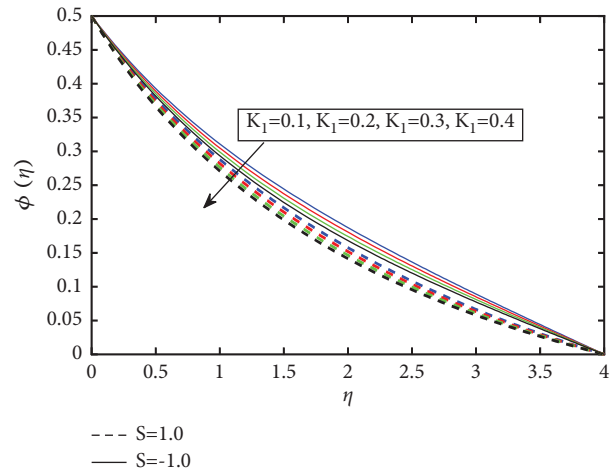
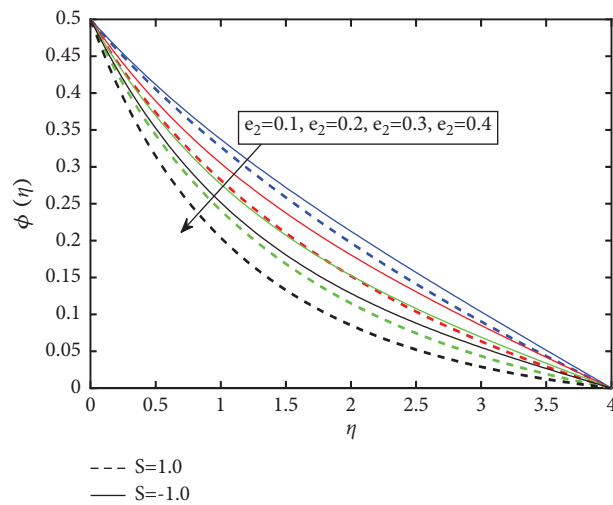
FIGURE 15: Outcome of Sc on concentration profiles.FIGURE 16: Outcome of K_1 on concentration profiles.FIGURE 17: Outcome of e_2 on concentration profiles.

TABLE 1: Values of $-\theta'(0)$ for several values of Prandtl number Pr.

Pr	Ananthaswamy et al. [39] with $St = 0 = Q_H$	Bidin and Nazar [44] with $E = 0 = K$	Mukhopadhyay [45] with $St = 0 = S = M$	Present study with $Wi = S = M = \lambda_2 = \gamma = e_1 = 0$
1.0	0.9548	0.9547	0.9547	0.95483
2.0	1.4715	1.4714	1.4714	1.47144
3.0	1.8691	1.8961	1.8961	1.89623

TABLE 2: The values of the skin friction coefficient, Nusselt number, and Sherwood number for various values of $Wi, M, \lambda_2, Pr, e_1, \gamma, Sc, K_1, e_2, S$.

Wi	M	λ_2	Pr	e_1	γ	Sc	K_1	e_2	S	$f''(0)$	$-\theta'(0)$	$-\phi'(0)$
0.1										-2.227621	1.153913	0.840286
0.4										-0.388551	1.136152	0.835266
	0.3									-2.562533	1.146825	0.838292
	0.5									-2.658439	1.144531	0.837647
		0.2								-2.562533	1.146825	0.838292
		0.5								-2.706850	1.143403	0.837330
			0.5							-2.562533	1.011794	0.838292
			0.7							-2.562533	1.146825	0.838292
				0.3						-2.562533	0.882451	0.838292
				0.5						-2.562642	0.652202	0.838291
					0.2					-2.562533	0.882451	0.838292
					0.4					-2.562533	0.868783	0.838292
						0.2				-2.562533	0.882451	0.838292
						0.5				-2.562533	0.882451	1.055563
							0.2			-2.562533	0.882451	0.838292
							0.4			-2.562533	0.882451	0.847343
								0.3		-2.562533	0.882451	0.838292
								0.5		-2.562533	0.882452	0.613178
									-1.0	-1.06091	0.691288	0.712030
									1.0	-2.562533	0.882451	0.838292

Prandtl number causes a significant decrease in fluid temperature and a thinning of the thermal boundary layer. When a sheet is stretched, this does not happen, but when a sheet is shrunk, an enormous Pr, fluid causes thermal unsteadiness at the superficial (i.e., a negative value of Nu), Figure 12 illustrates this effects.

Figure 13 displays the temperature profile's response to increasing and decreasing the thermal stratification parameter. As becomes larger e_1 , the temperature profile flattens out. Physically, a high level of thermal stratification reduces the difference in temperature between the surface and the surrounding air. Changing the heat generation/absorption parameter γ results in a corresponding change in temperature, as seen in Figure 14. It has been determined that there is an upward trend in the temperature profile.

See Figures 15–17 for visual representations of the fluid concentration's sensitivity to changes in the Schmidt number, the chemical reaction parameter, and the solutal stratification parameter. The concentration characteristics and the concentration border thickness decrease as Sc, K_1 and e_2 augment together with the mass transfer rate. It follows that the solutal boundary layer grows as a result of both heat diffusion and constructive reaction. The solutal

stratification parameter is the outcome of the possibility of a lower concentration of fluid near the plate than in the surrounding medium.

6. Conclusions

The current work provides the Williamson fluid flow in the presence of a chemical reaction via a permeable stretching/shrinking sheet in the MHD boundary layer. This work is innovative in that it uses thermal radiation to examine the physical consequences of thermal and solutal stratification on mass transport and convective heat. The Williamson fluid model introduces non-Newtonian behavior, and exploring how the rheological properties influence the flow and heat transfer can be a novel aspect. Understanding how shear-thinning behavior affects the velocity and temperature profiles would be valuable. Interesting discoveries, such as how these dual gradients impact heat transport close to the shrinking/stretching sheet, may result from the double stratification. In applications involving industrial or environmental processes, this element can be especially important. The governing equations have been converted via dimensionless transformations into a set of nonlinear

ordinary differential equations, which are then numerically solved using the BVP4c technique. The effects of some regulating factors were examined and visually shown. Our numerical findings lead to the following conclusions:

- (i) A decline in the dimensionless velocity and an improvement in the temperature and concentration profiles lead to an increase in the permeability, magnetic, and Williamson properties
- (ii) The temperature of a fluid decreases as its Prandtl number rises and vice versa
- (iii) By contrast, the heat generation/absorption parameter has the opposite impact on the temperature profile when it is increased
- (iv) The Schmidt number, solutal stratification parameter, and chemical reaction parameter are all impacted by fluid concentration. Concentration characteristics and border thickness decrease with increasing Sc and K_1
- (v) The temperature and local Nusselt numbers are reduced when the thermal stratification parameter e_1 is present
- (vi) Increasing values of the solutal stratification parameter e_2 lead to a decrease in the concentration and Sherwood numbers

Nomenclature

a_1, a_2, b_1, b_2 :	Constants
u :	Velocity component in the x direction
v :	Velocity component in the y direction
C :	Dimensional concentration of the fluid
C_∞ :	Concentration of the free stream
C_w :	Concentration at the surface
c_p :	Specific heat capacity at constant pressure
D :	Specifies diffusivity
T :	Dimensional temperature of the fluid
T_w :	Temperature at the surface
T_∞ :	Temperature of the free stream
B :	Magnetic field strength
$f'(\eta)$:	Nondimensional velocity
S :	Suction/ injection
Q :	Heat generation or absorption coefficient
$h(\eta)$:	Nondimensional concentration
k_r :	Dimensional chemical reaction parameter
K_1 :	Nondimensional chemical reaction parameter
M :	Nondimensional magnetic parameter
Pr :	Prandtl number
Sc :	Schmidt number
e_1 :	Thermal stratification parameter
e_2 :	Solutal stratification parameter
k' :	Darcy permeability of the porous medium
Wi :	Non-Newtonian Williamson parameter

Greek Symbols

$\theta(\eta)$:	Nondimensional temperature
η :	Similarity variable
λ_2 :	Permeability parameter

σ :	Electrical conductivity
γ :	Heat generation/absorption parameter
Γ :	Williamson time constant
ψ :	Stream function
ρ :	Density of the fluid
ν :	Kinematic viscosity
μ :	Dynamic viscosity

Subscripts

∞ :	Condition at the free stream
w :	Condition at the surface.

Data Availability

The data used to support the findings of this study are available from the corresponding author upon request.

Conflicts of Interest

The authors declare that they have no conflicts of interest.

References

- [1] S. Nadeem and N. Sher Akbar, "Effects of heat and mass transfer peristaltic flow of Williamson fluid in a vertical annulus," *Meccanica*, vol. 47, no. 1, pp. 141–151, 2012.
- [2] K. Vajravelu, S. Sreenadh, K. Rajanikanth, and C. Lee, "Peristaltic transport of a Williamson fluid in asymmetric channels with permeable walls," *Nonlinear Analysis: Real World Applications*, vol. 13, no. 6, pp. 2804–2822, 2012.
- [3] I. Dapra and G. Scarpi, "Perturbation solution for pulsatile flow of a non-Newtonian Williamson fluid in a rock fracture," *International Journal of Rock Mechanics and Mining Sciences*, vol. 44, no. 2, pp. 271–278, 2007.
- [4] N. A. Khan and H. Khan, "A boundary layer flows of non-Newtonian Williamson fluid," *Nonlinear Engineering*, vol. 3, no. 2, pp. 107–115, 2014.
- [5] S. Nadeem, S. T. Hussain, and C. Lee, "Flow of a Williamson fluid over a stretching sheet," *Brazilian Journal of Chemical Engineering*, vol. 30, no. 3, pp. 619–625, 2013.
- [6] T. Hayat, U. Khalid, and M. Qasim, "Steady flow of a Williamson fluid past a porous plate," *Asia-Pacific Journal of Chemical Engineering*, vol. 7, no. 2, pp. 302–306, 2012.
- [7] R. Bandi, S. Babu Mallela, S. Sreedharamalle, and D. Putta, "The flow of non-Newtonian fluid in an inclined channel through variable permeability," *Heat Transfer*, vol. 52, no. 4, pp. 3058–3073, 2023.
- [8] M. Sudheer Babu, B. Reddappa, and K. A. Ajmath, "Chemical reaction effects on MHD heat and mass transfer of a Jeffrey fluid flow with viscous dissipation and joule heating through a porous stretching sheet," *ARPJ Journal of Engineering and Applied Sciences*, vol. 18, no. 2, pp. 102–112, 2023.
- [9] R. Y. Jumah and A. S. Mujumdar, "Free convection heat and mass transfer of non-Newtonian power law fluids with yield stress from a vertical flat plate in saturated porous media," *International Communications in Heat and Mass Transfer*, vol. 27, no. 4, pp. 485–494, 2000.
- [10] P. V. S. N. Murthy, D. Srinivasacharya and, and P. V. S. S. R. Krishna, "Effect of double stratification on free convection in a darcian porous medium," *Journal of Heat Transfer*, vol. 126, no. 2, pp. 297–300, 2004.

- [11] P. A. Lakshmi Narayana and P. V. S. N. Murthy, "Free convective heat and mass transfer in a doubly stratified non-Darcy porous medium," *Journal of Heat Transfer*, vol. 128, no. 11, pp. 1204–1212, 2006.
- [12] C. Y. Cheng, "Combined heat and mass transfer in natural convection flow from a vertical wavy surface in a power-law fluid saturated porous medium with thermal and mass stratification," *International Communications in Heat and Mass Transfer*, vol. 36, no. 4, pp. 351–356, 2009.
- [13] P. A. L. Narayana, P. V. S. N. Murthy, P. V. S. S. R. Krishna, and A. Postelnicu, "Free convective heat and mass transfer in a doubly stratified porous medium saturated with a power-law fluid," *International Journal of Fluid Mechanics Research*, vol. 36, no. 6, pp. 524–537, 2009.
- [14] B. Lavanya and A. Leela Ratnam, "Effects of thermal radiation, heat generation, viscous dissipation and chemical reaction on MHD micropolar fluid past a stretching surface in a non-darcian porous medium," *Global journal of Engineering, design and technology*, vol. 3, no. 4, pp. 28–40, 2014.
- [15] C. Li, J. Huang, Y. Shang, and H. Huang, "Study on the flow and heat dissipation of water-based alumina nanofluids in microchannels," *Case Studies in Thermal Engineering*, vol. 22, 2020.
- [16] D. Srinivasacharya and G. Swamy Reddy, "Chemical reaction and radiation effects on mixed convection heat and mass transfer over a vertical plate in power-law fluid saturated porous medium," *Journal of the Egyptian Mathematical Society*, vol. 24, no. 1, pp. 108–115, 2016.
- [17] H. Bhowmik, A. Gharibi, A. Yaarubi, and N. Alawi, "Transient natural convection heat transfer analyses from a horizontal cylinder," *Case Studies in Thermal Engineering*, vol. 14, 2019.
- [18] S. Jena, G. C. Dash, and S. R. Mishra, "Chemical reaction effect on MHD viscoelastic fluid flow over a vertical stretching sheet with heat source/sink," *Ain Shams Engineering Journal*, vol. 9, no. 4, pp. 1205–1213, 2018.
- [19] M. A. Kumar, Y. D. Reddy, B. S. Goud, and V. S. Rao, "Effects of solet, dufour, hall current and rotation on MHD natural convective heat and mass transfer flow past an accelerated vertical plate through a porous medium," *International Journal of Thermofluids*, vol. 9, 2021.
- [20] B. S. Goud, Y. D. Reddy, V. S. Rao, and Z. H. Khan, "Thermal radiation and Joule heating effects on a magnetohydrodynamic Casson nanofluid flow in the presence of chemical reaction through a non-linear inclined porous stretching sheet," *Journal of Naval Architecture and Marine Engineering*, vol. 17, no. 2, pp. 143–164, 2020.
- [21] Y. D. Reddy, V. S. Rao, and M. A. Kumar, "Effect of heat generation/absorption on MHD copper-water nanofluid flow over a non-linear stretching/shrinking sheet," *AIP Conference Proceedings*, vol. 2246, 2020.
- [22] Y. D. Reddy, V. S. Rao, D. Ramya, and L. A. Babu, "MHD boundary layer flow of nanofluid and heat transfer over a nonlinear stretching sheet with chemical reaction and suction/blowing," *Journal of Nanofluids*, vol. 7, no. 2, pp. 404–412, 2018.
- [23] Y. Reddy, V. Rao, and L. Babu, "MHD boundary layer flow of nanofluid and heat transfer over a porous exponentially stretching sheet in presence of thermal radiation and chemical reaction with suction," *International Journal of Mathematics Trends and Technology*, vol. 47, no. 2, pp. 87–100, 2017.
- [24] Y. D. Reddy, D. Ramya, and L. A. Babu, "Effect of thermal radiation on MHD boundary layer flow of nanofluid and heat transfer over a non-linearly stretching sheet with transpiration," *Journal of Nanofluids*, vol. 5, no. 6, pp. 889–897, 2016.
- [25] Y. Dharmendar Reddy, V. S. Rao, and L. Anand Babu, "Viscous dissipation and partial slip effects on mhd boundary layer flow of nanofluid and heat transfer over A nonlinear stretching sheet with non-uniform heat source," *International Journal of Mathematical Archive*, vol. 8, no. 8, 2017.
- [26] R. Srinivasa Raju, M. Anil Kumar, and Y. Dharmendar Reddy, "Unsteady MHD free convective flow past a vertical porous plate with variable suction," *ARP Journal of Engineering and Applied Sciences*, vol. 11, no. 23, pp. 13608–13616, 2016.
- [27] R. Al-Ajmi and M. Mosaad, "Heat exchange between film condensation and porous natural convection across a vertical wall," *Fluid Dynamics and Materials Processing*, vol. 8, no. 1, pp. 51–68, 2012.
- [28] S. Hamimid, M. Guellal, A. Amroune, and N. Zeraibi, "Effect of a porous layer on the flow structure and heat transfer in a square, cavity," *Fluid Dynamics and Materials Processing*, vol. 8, no. 1, pp. 69–90, 2012.
- [29] K. Choukairy and R. Bennacer, "Numerical and analytical analysis of the thermosolutal convection in an heterogeneous porous cavity. Fluid Dyn," *Materialen en Processen*, vol. 8, no. 2, pp. 155–173, 2012.
- [30] N. Labeled, L. Bennamoun, and J. P. Fohr, "Experimental study of two-phase flow in porous media with measurement of relative permeability," *Fluid Dynamics and Materials Processing*, vol. 8, no. 4, pp. 423–436, 2012.
- [31] P. Ram and A. Bhandari, "Flow characteristics of revolving ferrofluid with variable viscosity in a porous medium in the presence of stationary disk," *Fluid Dynamics and Materials Processing*, vol. 9, no. 4, pp. 437–452, 2012.
- [32] B. Reddappa, M. Sudheer Babu, and S. Sreenadh, "MHD free convection and the effects of second order chemical reactions and double stratification Jeffrey flow through porous medium over an exponentially stretching sheet," *ARP Journal of Engineering and Applied Sciences*, vol. 17, no. 10, 2012.
- [33] M. R. Krishnamurthy, B. C. Prasannakumara, B. J. Gireesha, and R. S. R. Gorla, "Effect of chemical reaction on MHD boundary layer flow and melting heat transfer of Williamson nanofluid in porous medium," *Engineering Science and Technology, an International Journal*, vol. 19, no. 1, pp. 53–61, 2016.
- [34] P. M. Krishna, Ch. Ramreddy, and C. V. Rao, "Effects of Double Stratification on MHD flow and heat transfer of nanofluid along a Permeable Vertical plate," *International Journal of Mathematical, Engineering and Management Sciences*, vol. 4, no. 6, pp. 1362–1372, 2019.
- [35] A. A. Khan, S. F. Sufahani, K. Zaimi, and M. Ferdows, "MHD flow and heat transfer of double stratified micropolar fluid over a vertical permeable shrinking/stretching sheet with chemical reaction and heat source," *Journal of Advanced Research in Applied Sciences and Engineering Technology*, vol. 21, no. 1, pp. 1–14, 2020.
- [36] R. R. Chetteti and A. Srivastav, "Double stratification in the flow of a Newtonian fluid along an inclined permeable stretching surface," *Advances in Modelling and Analysis A*, vol. 58, no. 1–4, pp. 1–5, 2021.
- [37] N. S. Yousef, A. M. Megahed, N. I. Ghoneim, M. Elsafi, and E. Fares, "Chemical reaction impact on MHD dissipative Casson-Williamson nanofluid flow over a slippery stretching sheet through porous medium," *Alexandria Engineering Journal*, vol. 61, no. 12, pp. 10161–10170, 2022.
- [38] S. Shaheen, M. B. Arain, K. S. Nisar, A. Ashwag, and S. h Md, "Fouad Othman Mallawi A case study of heat transmission in a Williamson fluid flow through a ciliated porous channel:

- a semi-numerical approach,” *Case Studies in Thermal Engineering*, vol. 41, pp. 1–10, 2023.
- [39] V. Ananthaswamy, R. R. Subanya, and S. Sivasankari, “A mathematical study on a steady MHD flow in double stratification medium,” *CFD Letters*, vol. 15, no. 10, pp. 34–51, 2023.
- [40] M. Umar, R. Akhtar, Z. Sabir et al., “Numerical treatment for the three-dimensional Eyring-Powell fluid flow over a stretching sheet with velocity slip and activation energy,” *Advances in Mathematical Physics*, vol. 2019, pp. 1–12, Article ID 9860471, 2019.
- [41] A. M. Megahed, “Williamson fluid flow due to a nonlinearly stretching sheet with viscous dissipation and thermal radiation,” *Journal of the Egyptian Mathematical Society*, vol. 27, 2019.
- [42] N. N. Reddy, V. S. Rao, and B. R. Reddy, “Chemical reaction impact on MHD natural convection flow through porous medium past an exponentially stretching sheet in presence of heat source/sink and viscous dissipation,” *Case Studies in Thermal Engineering*, vol. 25, 2021.
- [43] S. Nadeem and S. T. Hussain, “Flow and heat transfer analysis of Williamson nanofluid,” *Applied Nanoscience*, vol. 4, no. 8, pp. 1005–1012, 2014.
- [44] B. Bidin and R. Nazar, “Numerical solution of the boundary layer flow over an exponentially stretching sheet with thermal radiation,” *European Journal of Scientific Research*, vol. 33, no. 4, pp. 710–717, 2009.
- [45] S. Mukhopadhyay, “MHD boundary layer flow and heat transfer over an exponentially stretching sheet embedded in a thermally stratified medium,” *Alexandria Engineering Journal*, vol. 52, no. 3, pp. 259–265, 2013.